Kinetic Mechanism of the GCN5-Related Chromosomal Aminoglycoside Acetyltransferase AAC(6′)-Ii from *Enterococcus faecium*: Evidence of Dimer Subunit Cooperativity†

Kari-ann Draker,‡ Dexter B. Northrop,§ and Gerard D. Wright*,‡

Antimicrobial Research Centre, Department of Biochemistry, McMaster University, 1200 Main Street West, Ontario L8N 3Z5, Canada, and Division of Pharmaceutical Sciences, School of Pharmacy, 777 Highland Avenue, University of Wisconsin−Madison, Madison, Wisconsin 53705

Received January 24, 2003; Revised Manuscript Received April 10, 2003

ABSTRACT: The aminoglycoside 6′-*N*-acetyltransferase AAC(6′)-Ii from *Enterococcus faecium* is an important microbial resistance determinant and a member of the GCN5-related *N*-acetyltransferase (GNAT) superfamily. We report here the further characterization of this enzyme in terms of the kinetic mechanism of acetyl transfer and identification of rate-contributing step(s) in catalysis, as well as investigations into the binding of both acetyl-CoA and aminoglycoside substrates to the AAC(6′)-Ii dimer. Product and dead-end inhibition studies revealed that AAC(6′)-Ii follows an ordered bi-bi ternary complex mechanism with acetyl-CoA binding first followed by antibiotic. Solvent viscosity studies demonstrated that aminoglycoside binding and product release govern the rate of acetyl transfer, as evidenced by changes in both the k_{cat}/K_b for aminoglycoside and k_{cat}, respectively, with increasing solvent viscosity. Solvent isotope effects were consistent with our viscosity studies that diffusion-controlled processes and not the chemical step were rate-limiting in drug modification. The patterns of partial and mixed inhibition observed during our mechanistic studies were followed up by investigating the possibility of subunit cooperativity in the AAC-(6′)-Ii dimer. Through the use of AAC-Trp^{164} → Ala, an active mutant which exists as a monomer in solution, the partial nature of the competitive inhibition observed in wild-type dead-end inhibition studies was alleviated. Isothermal titration calorimetry studies also indicated two nonequivalent antibiotic binding sites for the AAC(6′)-Ii dimer but only one binding site for the Trp^{164} → Ala mutant. Taken together, these results demonstrate subunit cooperativity in the AAC(6′)-Ii dimer, with possible relevance to other oligomeric members of the GNAT superfamily.

Aminocyclitol−aminoglycoside antibiotics are a class of bactericidal drugs used in the treatment of infections caused by various Gram-positive and Gram-negative bacteria. Clinically relevant resistance to the aminoglycosides is mediated by the action of enzymes that modify the drugs and decrease their affinity for the 30S ribosomal subunit target (*1*, *2*). Aminoglycoside-inactivating enzymes include the phosphotransferase (APH),[1] nucleotidylyltransferase (ANT), and acetyltransferase (AAC) proteins, which are responsible for O-phosphorylation, O-adenylation, and N- or O-acetylation of the drugs, respectively (reviewed in refs *3* and *4*).

N-Acetylation at the 6′ position of aminoglycosides is one of the most prevalent forms of modification in Gram-negative bacteria (*3*). To date, only two AAC(6′) enzymes from Gram-positive pathogens have been identified and characterized: the bifunctional AAC(6′)-APH(2″) protein from enterococci and staphylococci (*4*) and AAC(6′)-Ii from *Enterococcus faecium* (*5*). The presence of these resistance determinants in enterococci complicates the use of β-lactam/aminoglycoside combination therapy in clinical treatment (*6*−*9*) and thus increases the reliance on other antimicrobials such as glycopeptides. As such, these proteins are worthy of study to both better understand the resistance they confer and apply this knowledge to the identification and/or design of enzyme inhibitors. The focus of this report is the further kinetic characterization of the aminoglycoside 6′-*N*-acetyltransferase, AAC(6′)-Ii.

The *aac(6′)-Ii* gene from *E. faecium* is chromosomal in origin and has been shown to confer low-level aminoglycoside resistance in vivo (*6*). Initial characterization of purified AAC(6)-Ii by Wright and Ladak (*5*) revealed that the protein is a homodimer in solution with a broad substrate specificity for several aminoglycosides of the 4,5- and 4,6-disubstituted deoxystreptamine class (see Figure 1) and specificity constants (k_{cat}/K_m) on the order of 10^4 M^{-1} s^{-1}.

The crystal structure of the AAC(6′)-Ii monomer in complex with acetyl-coenzyme A was solved by Berghuis and co-workers in 1999 (*10*), who identified it as a member of the GCN5-related *N*-acetyltransferase (GNAT) superfamily (*11*). This family of diverse enzymes is defined by several conserved sequence motifs involved in the binding of the common acyl-coenzyme A substrate. Several recent crystal structures of various GNAT enzymes such as transcription

† This work was supported by Canadian Institutes of Health Research Grant MT-13536.

* To whom correspondence should be addressed. Tel: 905-525-9140 (ext 22454). Fax: 905-522-9033. E-mail: wrightge@mcmaster.ca.

‡ McMaster University.

§ University of Wisconsin−Madison.

[1] Abbreviations: APH, aminoglycoside phosphotransferase; ANT, aminoglycoside nucleotidylyltransferase; AAC, aminoglycoside acetyltransferase; WT, wild type; ITC, isothermal titration calorimetry; GNAT, GCN5-related *N*-acetyltransferase.

10.1021/bi034148h CCC: $25.00
Published on Web 05/06/2003

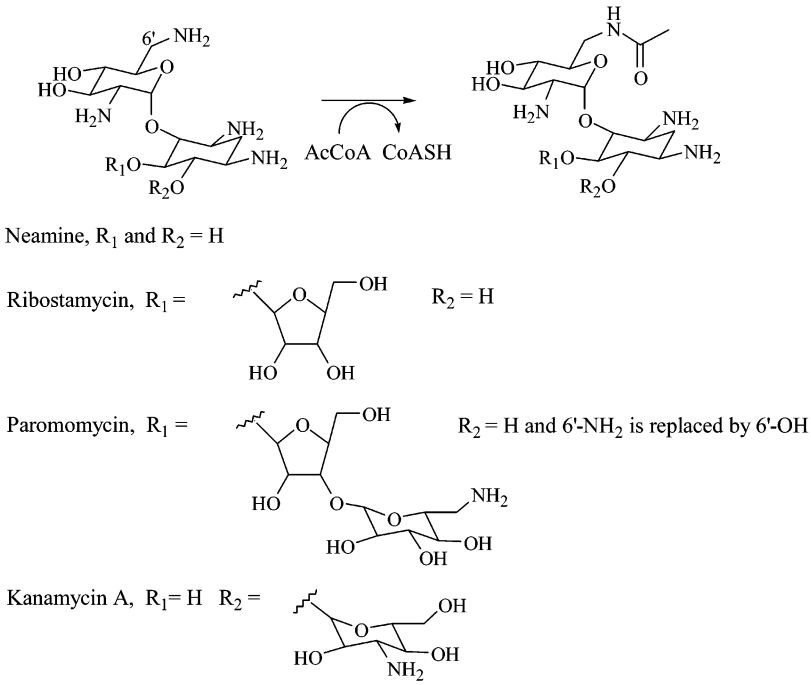

FIGURE 1: Regiospecific acetyl-transfer reaction catalyzed by AAC(6′)-Ii and structures of aminoglycosides used in this study.

factor/histone acetyltransferases (*12*−*16*), arylamine/arylalkylamine acetyltransferases (*17*−*20*), and *N*-myristoyltransferases (*18*, *21*), as well as sugar (*22*) and aminoglycoside acetyltransferases (*10*, *23*), reveal the striking structural homology shared among the superfamily members (reviewed in ref *43*). In addition to structural homology, AAC(6′)-Ii has also been shown to be a functional homologue of histone acetyltransferases, revealed by its capacity to modify histones as well as other small basic proteins (*10*).

Several detailed kinetic analyses have been done to better characterize the mechanism of group transfer by many GNAT superfamily members (*24*−*27*), as well as a limited number of studies on bacterial aminoglycoside acetyltransferases (*28*−*31*). Our level of understanding of the molecular mechanism of AAC(6′)-Ii, however, is superficial, and we therefore report here a series of mechanistic studies on this enzyme to determine the kinetic mechanism of catalysis and to identify the rate-determining steps of acetyl transfer. Additional studies with a monomeric form of the enzyme and isothermal titration calorimetry (ITC) experiments further defined the mechanism of acetyl transfer by AAC(6′)-Ii and provide insight into the physiological homodimeric form of AAC(6′)-Ii. Our results allow us to compare the mechanism of acetylation by this resistance determinant with other bacterial AACs as well as with other members of the GNAT superfamily.

MATERIALS AND METHODS

General. Aminoglycosides, desulfo-coenzyme A, and 4,4-dithiodipyridine were from Sigma-Aldrich Chemical Co. (St. Louis, MO). The *aac(6′)-Ii* gene was subcloned from the pPLaac vector (*5*) into pET22b(+) (Novagen, Madison, WI) using the flanking *Nde*I and *Hin*dIII restriction sites. AAC(6′)Ii was subsequently overexpressed in *Escherichia coli* BL21(DE3) cells and purified to homogeneity following the procedures outlined previously (*5*).

AAC(6′)-Ii Kinetic Assays. Protein acetyltransferase activity was monitored with a continuous assay by the in situ titration of coenzyme A product with 4,4-dithiodipyridine at 324 nm, as previously described (*5*, *32*).

Initial Velocity Experiments. Initial rate data for AAC(6′)-Ii acetylation of ribostamycin were collected at various concentrations of both acetyl-CoA and aminoglycoside. The data were fit by nonlinear least-squares fit to global eq 1 using Grafit software (*33*). The equation describes a sequential, ternary complex mechanism, where [A] and [B] are the concentrations of substrates, K_a and K_b are the respective Michaelis−Menten constants, and K_{ia} is the dissociation constant for A:

$$v = V_{max}[A][B]/(K_{ia}K_b + K_b[A] + K_a[B] + [A][B]) \quad (1)$$

AAC(6′)-Ii Inhibition Studies. AAC(6′)-Ii acetyltransferase activity was monitored in the presence of the dead-end inhibitors desulfo-CoA and paromomycin or the product inhibitor 6′-N-acetylated ribostamycin. Individual rate data generated at various concentrations of inhibitor were first fit to eq 2 describing Michaelis−Menten kinetics using Grafit 4.0 software (*33*):

$$v = V_{max}[S]/(K_m + [S]) \quad (2)$$

Reciprocal plots of each data set were then generated and are presented in Figures 3−5. Kinetic constants included in Table 1 are derived from the fit of the data to global equations of best fit describing either partially competitive inhibition (eq 3), uncompetitive inhibition (eq 4), or noncompetitive/mixed inhibition (eq 5) by nonlinear least squares using the enzyme kinetics module of Sigma Plot (*34*):

$$v = V_{max}[S]/(K_m((1 + I/K_{ii})/(1 + I/K_{is})) + [S]) \quad (3)$$

$$v = V_{max}[S]/(K_m + [S](1 + I/K_{ii})) \quad (4)$$

$$v = V_{max}[S]/(K_m(1 + I/K_{is}) + [S](1 + I/K_{ii})) \quad (5)$$

Table 1: Summary of AAC(6′)-Ii Dead-End and Product Inhibition Studies

inhibitor	varied substrate	fixed substrate	pattern of inhibition	K_{is} (μM)[a]	K_{ii} (μM)[b]
desulfo-CoA	acetyl-CoA	ribostamycin (200 μM)	partially competitive	6.58 ± 2.18	24.3 ± 8.9
desulfo-CoA	ribostamycin	acetyl-CoA (50 μM)	noncompetitive/mixed	81.3 ± 42.1	99.0 ± 34
paromomycin	acetyl-CoA	ribostamycin (100 μM)	uncompetitive		180 ± 13
AcRibo	ribostamycin	acetyl-CoA (100 μM)	noncompetitive/mixed	45.9 ± 14.1	363 ± 190
AcRibo	acetyl-CoA	ribostamycin (20 μM)	no inhibition[c]		

[a] K_{is}, $K_{i(slope)} = \alpha K_i$, where α is the factor by which K_m changes when I is bound to the ES complex. [b] K_{ii}, $K_{i(intercept)} = K_i$. [c] See text for details.

Alternative Substrate Method. To verify the kinetic mechanism of AAC(6′)-Ii determined by our inhibitor studies, alternative substrate studies described by Radika and Northrop (*35*) were performed. Briefly, initial rate data were collected at varying concentrations of acetyl-CoA (5−250 μM) using saturating concentrations (>10K_m) of neomycin, ribostamycin, butirosin, neamine, or amikacin. Data were fit to eq 2 and reciprocal plots of $1/v$ vs 1/[acetyl-CoA] for each alternate aminoglycoside used in the diagnostic.

Enzymatic Synthesis of 6′-N-Acetylated Ribostamycin. 6′-N-Acetylated ribostamycin (AcRibo) was enzymatically synthesized by AAC(6′)-Ii using acetyl-CoA and ribostamycin as aminoglycoside substrate. Synthesis of AcRibo was conducted using a 1:5 molar ratio of ribostamycin to acetyl-CoA and ca. 2 μmol of AAC(6′)-Ii enzyme. Reactions were carried out in water and incubated for 1 h at room temperature. AcRibo was separated from other components by applying the reaction mixture to a 2 mL column of Dowex analytical grade cation-exchanger resin AG 50W (Bio-Rad) equilibrated with H_2O, followed by elution at 2 M NH_2OH using a 1 M stepwise gradient from 1 to 5 M NH_2OH. The progress of AcRibo formation and separation from other reaction components was monitored by thin-layer chromatography (TLC) using 250 μm silica G plates and a 5:2 ratio of MeOH:NH_4OH as the solvent system. Distinct spots for AcRibo ($R_f = 0.30$) and ribostamycin controls ($R_f = 0.12$) were visualized by ninhydrin spray, and CoA product ($R_f = 0.53$) was visualized under UV light. The identity of the isolated product as 6′-N-acetylated ribostamycin was confirmed by electrospray mass spectrometry as well as proton and ^{13}C NMR.

Viscosity Studies. AAC(6′)-Ii kinetic assays were performed with the macroviscosogen PEG 8000 (6.7%) and the microviscosogen sucrose (0−30%). The viscosity of solutions was determined in quadruplicate at 22 °C using an Ostwald viscometer, relative to the standard AAC(6′)-Ii kinetic buffer consisting of 25 mM MES, pH 6.0, and 1 mM EDTA. K_i determinations for the competitive inhibitor paromomycin were made in the presence of 30% microviscosogen to ensure that the reagents were not binding to the enzyme active site. Enzyme assays were performed in duplicate in a final volume of 800 μL. Initial rate data were fit by nonlinear least-squares regression to eq 2 using Grafit 4.0 software (*33*). The values reported in Table 2 are the slopes of plots from either k_{cat}^0/k_{cat} or $(k_{cat}/K_m^0)/(k_{cat}/K_m)$ versus the relative viscosity of the solution.

AAC-Trp^{164} → Ala Monomer Mutant. The replacement of tryptophan at position 164 with alanine was performed using the QuikChange site-directed mutagenesis protocol (Stratagene) and the mutagenic oligonucleotide primers 5′ CTCAATACGGTATCACAGGTGCGGAATTGCATCC 3′ and 5′ GGATGCAATTCCGCACCTGTGATACCGTATTGAG 3′. The presence of the desired mutation in the *aac(6′)-Ii* gene as well as the absence of adventitious mutations was confirmed by complete gene sequencing at the Central Facility of the Institute for Molecular Biology and Biotechnology, McMaster University. Subsequent overexpression and purification of the AAC-Trp^{164} → Ala mutant, as well as the determination of kinetics of acetyl transfer to various aminoglycosides for this mutant, were the same as those described for the WT enzyme (*5*).

Table 2: Solvent Viscosity Effects on AAC(6′)-Ii Activity

viscosogen	varied substrate	fixed substrate	$(k_{cat}^0/k_{cat})^{\eta}$ [a]	$[(k_{cat}/K_m^0)/(k_{cat}/K_m)]^{\eta}$
PEG 8000	AcCoA	Kan A (200 μM)	0.023	−0.012
	Kan A	AcCoA (100 μM)	0.0044	−0.030
sucrose	AcCoA	Ribo (100 μM)	0.787	−0.012
	Kan A	AcCoA (100 μM)	0.425	1.090
	Ribo	AcCoA (100 μM)	0.521	0.716

[a] The values reported are the slopes of plots for k_{cat}^0/k_{cat} or $[(k_{cat}/K_m^0)/(k_{cat}/K_m)]$ versus the relative viscosity of the solution.

Analytical gel filtration experiments on AAC-Trp^{164} → Ala were used to confirm initial evidence that this mutant was a monomer in solution. AAC-Trp^{164} → Ala at ∼2.10 mg/mL was analyzed on an analytical Superdex 200 HR 10/30 column (Bio-Rad). A molecular mass calibration curve was generated using α-lactalbumin (14.2 kDa), carbonic anhydrase (29 kDa), chicken egg albumin (45 kDa), and BSA (66 kDa monomer, 132 kDa dimer) as well as Blue Dextran to determine the column void volume. The molecular masses of WT AAC(6′)-Ii and the Trp^{164} → Ala mutant were estimated using the formula $K_{av} = (V_e - V_0)/(V_t - V_0)$, where V_e is the protein elution volume from the column, V_t is the total column volume, and V_0 is the column void volume. From these analytical gel filtration experiments, the estimated molecular mass of WT AAC(6′)-Ii was ∼45900 Da and AAC-Trp^{164} → Ala ∼22900 Da, confirming the monomeric form of this mutant in solution.

Isothermal Titration Calorimetry Experiments. All ITC measurements were made using a MicroCal VP-ITC isothermal titration calorimeter from MicroCal, Inc. (Northampton, MA). A buffer solution of 25 mM HEPES, pH 7.5, and 2 mM EDTA was used to dialyze purified AAC(6′)-Ii WT or Trp^{164} → Ala enzyme and the resulting dialyzate used to make aminoglycoside and/or CoA solutions. In general, a 100 μM solution of AAC(6′)-Ii in 25 mM HEPES, pH 7.5, and 2 mM EDTA was added to the sample cell (ca. 1.4 mL), and a 0.5−2.0 mM solution of neamine, kanamycin A, or ribostamycin as titrant was loaded into the injection syringe. For each titration experiment, a 60 s delay at the start was followed by 29 injections of 10 μL of the titrant solution, spaced apart by 240 s. The sample cell was stirred at 300 rpm throughout and maintained at a temperature of 37 °C. Additional experiments were performed as described above

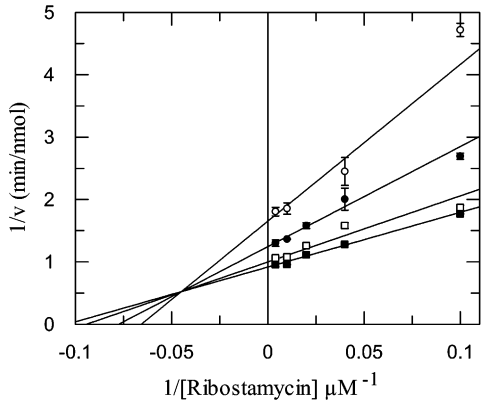

FIGURE 2: AAC(6′)-Ii initial velocity patterns. Double reciprocal plot of initial rate data at varying ribostamycin concentrations and fixed concentrations of acetyl-CoA at 5 μM (○), 10 μM (●), 25 μM (□), and 50 μM (■). The pattern of intersecting lines is indicative of a sequential kinetic mechanism. The best fit of the data to eq 1 gave kinetic constants of $K_a = 8.3 \pm 1.4$ μM, $K_b = 4.9 + 0.58$ μM, and $K_{ia} = 22 \pm 6.3$ μM.

in the presence of 2 mM coenzyme A in both the sample cell and injection syringe. Several control titrations were performed and included baseline titrations of buffer into enzyme, titrant solutions into buffer, and CoA titrated into an enzyme and CoA solution. Titration data were analyzed using Origin 5.0 software supplied by Microcal. Briefly, data sets were corrected for baseline heats of dilutions from blank or control runs as appropriate. Corrected data were then fit to a theoretical titration curve describing two independent sets of binding sites for titrant. Calculated K_a values with the smallest standard error gave an acceptable c value between 1 and 1000 (*36*). Free energies of association (ΔG) were calculated using the equation:

$$\Delta G = -RT \ln K_a \quad (6)$$

ITC experiments performed with the AAC-Trp^{164} → Ala monomer were as described for the WT enzyme and the data best fit to a theoretical titration curve describing one binding site for the aminoglycoside titrant.

RESULTS

Initial Velocity Studies. Initial velocity patterns obtained when the ribostamycin concentration was varied at various fixed concentrations of acetyl-CoA displayed intersecting lines in the double reciprocal plot (Figure 2), indicative of a ternary complex, sequential mechanism.

Inhibition Studies. To gain further insight into the mechanism of AAC(6′)-Ii acetyl transfer, desulfo-CoA and paromomycin were used as dead-end inhibitors to investigate the order of substrate binding and product release by the enzyme. Desulfo-CoA was chosen as the dead-end inhibitor as it does not interfere with the thiol titration assay, and the aminoglycoside paromomycin, which lacks a 6′-amino group, has already been shown to be a competitive inhibitor of AAC(6′)-Ii activity (*1*).

AAC(6′)-Ii acetyl-transfer kinetics in the presence of increasing concentrations of desulfo-CoA resulted in partial competitive inhibition of enzyme activity when acetyl-CoA was the varied substrate, with $K_{is} = 6.6$ μM and $K_{ii} = 24$ μM for the dead-end inhibitor (Figure 3A and Table 1). Noncompetitive/mixed-type inhibition was observed when the aminoglycoside ribostamycin was the variable substrate in desulfo-CoA inhibition studies. In the presence of a fixed subsaturating concentration of acetyl-CoA (50 μM), $K_{is} = 81$ μM and $K_{ii} = 99$ μM (Table 1).

We used the 6′-hydroxy aminoglycoside paromomycin as a dead-end inhibitor of AAC(6′)-Ii activity to further elucidate the kinetic mechanism. From the double reciprocal plot of $1/v$ versus 1/[acetyl-CoA] shown in Figure 4, paromomycin exhibits uncompetitive inhibition of AAC(6′)-Ii activity versus acetyl-CoA (Table 1). This pattern of inhibition indicates that paromomycin can bind to either the AAC(6′)-Ii·AcCoA binary complex or the AAC(6′)-Ii·CoA product complex, with paromomycin binding to the latter preventing the release of CoA and suggesting partial rate limitation by the dissociation of CoA from the enzyme. Our results are therefore consistent with ordered substrate addition and product release.

6′-N-Acetylated ribostamycin (AcRibo) used in product inhibition studies was found to be a noncompetitive/mixed-

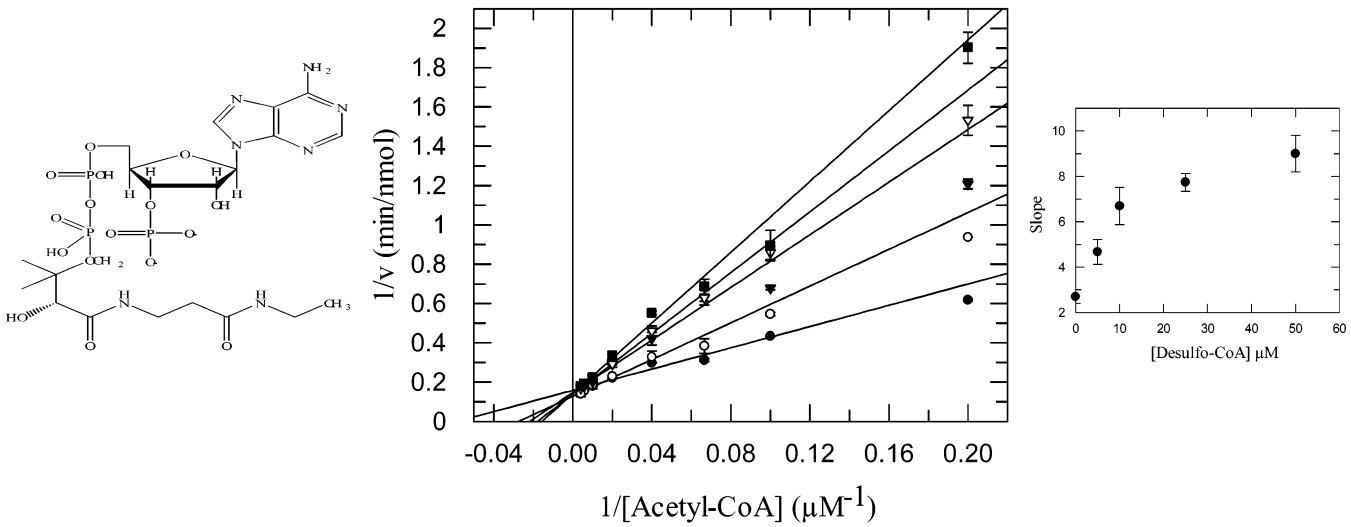

FIGURE 3: Partial competitive inhibition of AAC(6′)-Ii activity through the use of desulfo-CoA as a dead-end inhibitor. The structure of desulfo-CoA is shown at the left. Shown is a plot of $1/v$ versus 1/[acetyl-CoA] at fixed concentrations of 0 μM (●), 5 μM (○), 10 μM (▼), 25 μM (▽), and 50 μM (■) desulfo-CoA. Ribostamycin was present in the assays at a saturating concentration of 200 μM. Inset: Hyperbolic-shaped replot for acetyl-CoA versus [desulfo-CoA], indicating partial inhibition.

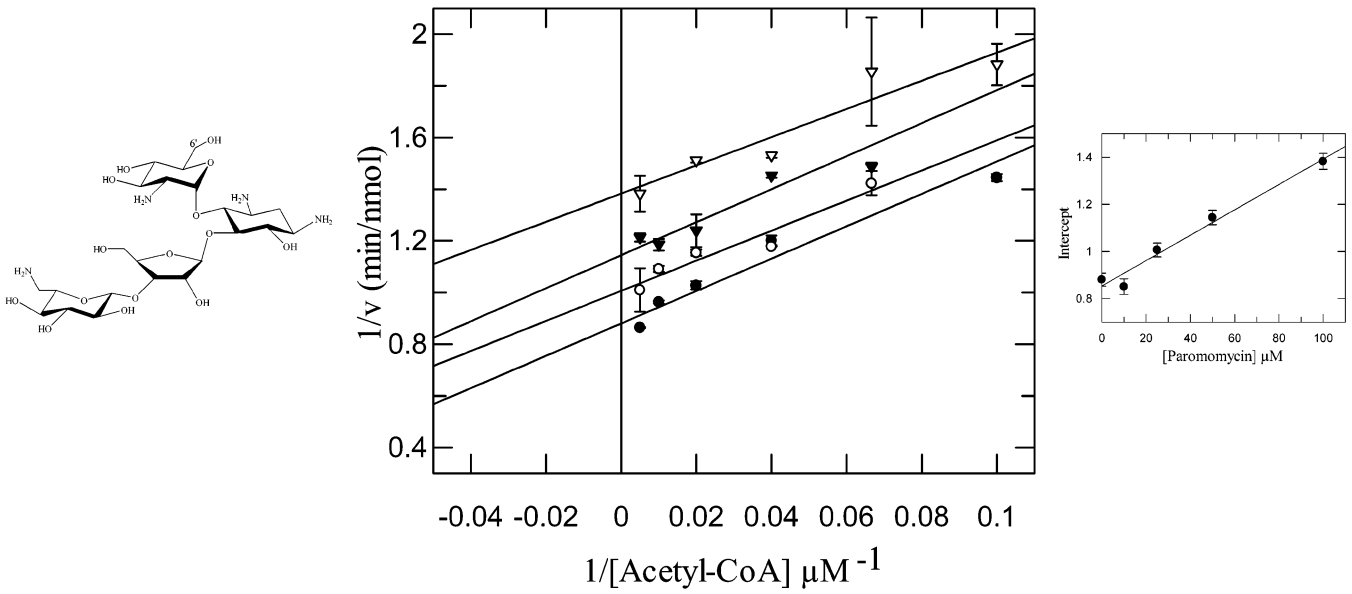

FIGURE 4: Uncompetitive inhibition of AAC(6′)-Ii activity through the use of paromomycin as a dead-end inhibitor. Plot of $1/v$ versus 1/[acetyl-CoA] at fixed concentrations of 0 μM (●), 25 μM (○), 50 μM (▼), and 100 μM (▽) paromomycin. Ribostamycin was present at a saturating concentration of 100 μM. Inset: Intercept and replot for acetyl-CoA versus [paromomycin].

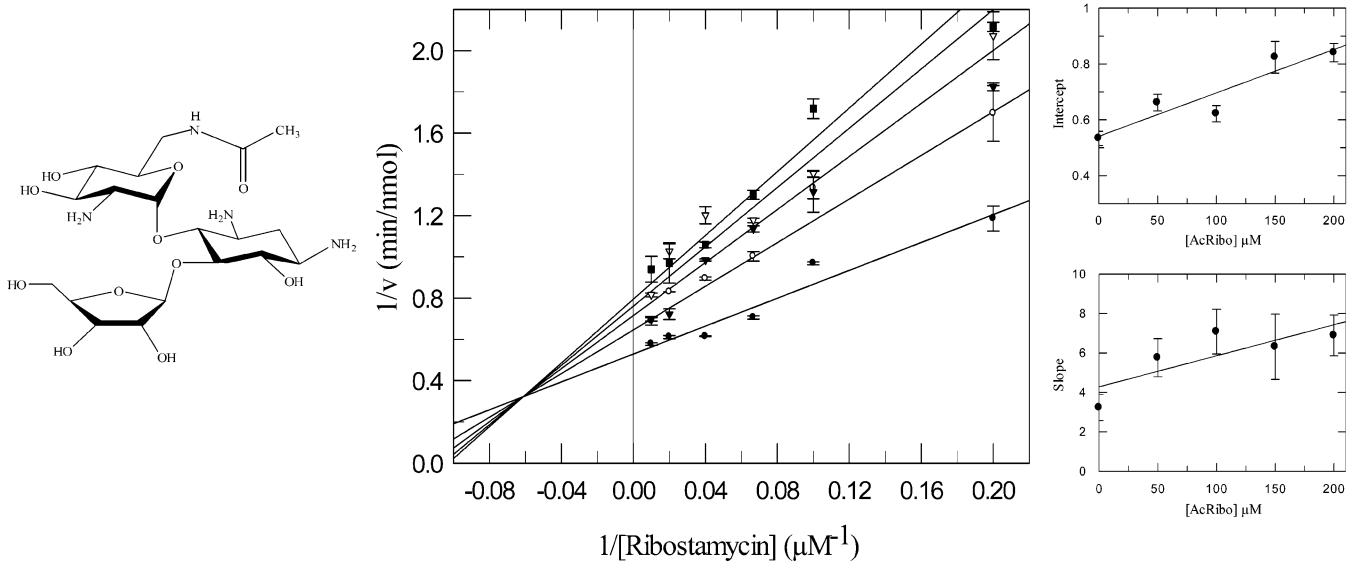

FIGURE 5: Mixed inhibition of AAC(6′)-Ii through the use of 6′-N-acetylated ribostamycin (AcRibo) as a product inhibitor. Double reciprocal plot of initial rate data at varying ribostamycin concentrations and fixed concentrations of AcRibo at 0 μM (●), 50 μM (○), 100 μM (▼), 150 μM (▽), and 200 μM (■). Acetyl-CoA was present at a saturating concentration of 100 μM. Inset: Intercept and slope replots for ribostamycin versus [AcRibo].

type inhibitor versus aminoglycoside substrate with K_{is} and K_{ii} values of 46 and 363 μM, respectively (Figure 5 and Table 1), indicative of AcRibo binding to the AAC(6′)-Ii·CoA complex. In addition, AcRibo did not behave as an inhibitor versus acetyl-CoA in the presence of either fixed subsaturating (20 μM) or fixed saturating (100 μM) concentrations of aminoglycoside. This lack of inhibition was evident even when AcRibo concentrations exceeded the fixed concentration of ribostamycin substrate by up to 50-fold. We hypothesize that AcRibo could behave as a noncompetitive inhibitor of acetyl-CoA at significantly higher concentrations that we could not achieve experimentally, which would be consistent with our dead-end inhibition. Our AcRibo inhibition results as a whole, however, support the kinetic mechanism and are consistent with the release of acetylated aminoglycoside first, followed by the slower release of the CoA product.

Scheme 1: AAC(6′)-Ii Follows an Ordered Bi-Bi Kinetic Mechanism[a]

[a] Abbreviations: AcCoA, acetyl-CoA; AG, aminoglycoside substrate; AcAG, acetylated aminoglycoside product.

Taken together, the results of product and dead-end inhibition studies (summarized in Table 1) indicate that AAC(6′)-Ii follows an ordered bi-bi reaction mechanism, as outlined in Scheme 1.

Alternative Substrate Diagnostic. Parallel patterns were obtained from double reciprocal plots of $1/v$ versus 1/[AcCoA] at saturating concentrations of numerous alternative

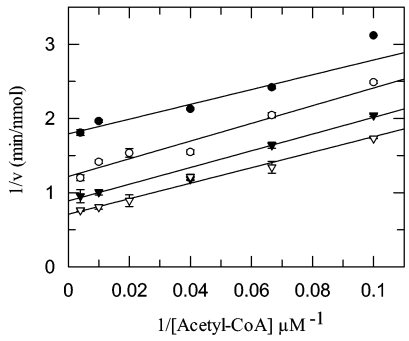

FIGURE 6: Alternate substrate diagnostic with acetyl-CoA as the variable substrate and fixed concentrations of aminoglycoside. Shown is a double reciprocal plot of $1/v$ versus 1/[acetyl-CoA] at fixed, saturating concentrations of neomycin (●), isepamicin (○), ribostamycin (▼), and butirosin (▽). Parallel lines are diagnostic of an ordered bi-bi kinetic mechanism.

aminoglycoside substrates (Figure 6). Thus, k_{cat}/K_a values determined for acetyl-CoA are independent of the aminoglycoside substrate, consistent with an ordered bi-bi mechanism (*35*) and our product and dead-end inhibition results.

Solvent Viscosity Effects. We also explored the rate-determining step(s) in AAC(6′)-Ii acetyl transfer using several approaches. Solvent viscosity effects on enzyme activity were first investigated to assess whether diffusion-controlled events such as product release may be rate-limiting. Using the microviscosogen sucrose, it was shown that there were significant solvent viscosity effects on AAC-(6′)-Ii activity (Table 2). As a control, the macroviscosogen PEG 8000 was shown to have no effect on enzyme activity, revealing that the rate changes observed in the presence of sucrose are effects on diffusion-controlled phenomenon and not the result of changes in global viscosity (*37*, *38*). In general, solvent viscosity effects describing k_{cat} changes ranged from 0.52 to 0.79 (Table 2), consistent with the suggestion that product release contributes significantly to the rate-determining step(s). In turn, the productive formation of the AAC·acetyl-CoA complex does not appear to be rate-limiting at all since virtually no viscosity effect was observed on k_{cat}/K_a values for acetyl-CoA (Table 2). The large k_{cat}/K_b changes observed when aminoglycoside is the varied substrate, however, do suggest that the productive formation of an enzyme complex with aminoglycoside may contribute to the rate-determining step(s). These results as a whole therefore indicate that diffusion-controlled events and not chemistry contribute to the rate-limiting step(s) in AAC(6′)-Ii acetyl transfer.

Solvent Isotope Effects. To confirm our solvent viscosity effects that chemistry is not rate-limiting in AAC(6′)-Ii acetyl transfer, we performed D_2O solvent isotope experiments to investigate the dependence of k_{cat} on proton abstraction at the 6′-amino group of an aminoglycoside substrate. Kinetic assays were performed in either 100% H_2O or ∼94% D_2O and a solvent isotope effect ($k_{cat}^{H/D}$ or $k_{cat}/K_m^{H/D}$) was determined. No significant solvent isotope effect was observed for ribostamycin or kanamycin, with $k_{cat}^{H/D}$ ranging from 1.1 to 1.3 and $k_{cat}/K_m^{H/D}$ from 1.1 to 1.4. In contrast, Benke-Marti (*39*) observed a solvent isotope effect on k_{cat}/K_m of 10 for the acetylation of tobramycin by AAC(3)-I, an enzyme that also follows an ordered bi-bi kinetic mechanism. The small effect that was observed for AAC(6′)-Ii may be attributed to the higher relative viscosity of D_2O compared to H_2O (*40*), supporting our argument for a diffusion-controlled process limiting AAC(6′)-Ii reaction rates.

Table 3: Steady-State Kinetic Parameters for Wild-Type and AAC-Trp^{164} → Ala Proteins[a]

substrate	K_m (μM)	k_{cat} (s^{-1})	k_{cat}/K_m (M^{-1} s^{-1})
	Wild Type[b]		
neamine	5.82 ±1.02	0.419 ± 0.020	7.2×10^4
kanamycin A	19.9 ± 8.84	0.816 ± 0.207	4.6×10^4
ribostamycin	9.08 ± 1.95	0.338 ± 0.220	3.7×10^4
neomycin C	5.31 ± 0.57	0.205 ± 0.0006	3.9×10^4
acetyl-CoA	23.5 ± 3.7	0.403 ± 0.025	1.7×10^4
	AAC-Trp^{164}→ Ala		
neamine	206 ± 32	0.048 ± 0.002	2.3×10^2
kanamycin A	280 ± 26	0.080 ± 0.0003	2.8×10^2
ribostamycin	217 ± 22	0.046 ± 0.001	2.1×10^2
neomycin C	23.7 ± 3.1	0.135 ± 0.001	5.7×10^3
acetyl-CoA	20.6 ± 2.3	0.173 ± 0.001	8.4×10^3

[a] Reactions were carried out at 37 °C in 25 mM MES (pH 6.0) and 1 mM EDTA. [b] Kinetic parameters for wild-type AAC(6′)-Ii are reproduced from ref *5*.

Studies on Monomeric AAC-Trp^{164} → Ala. Mutation of Trp^{164} to Ala resulted in an active enzyme with the characteristics of a monomer rather than a dimer, which is the native state of the enzyme. Trp^{164} is located in the C-terminal region of AAC(6′)-Ii and is relatively solvent exposed in the published crystal structure (*10*). Given that mutation of this residue blocks homodimer formation, we propose that this residue is involved in critical monomer−monomer interactions that are essential for dimer formation.

Activity of AAC-Trp^{164} → Ala. Steady-state kinetic analysis revealed that the AAC-Trp^{164} → Ala monomer retained the capacity to modify various aminoglycosides, including the minimal substrate neamine (*5*) as well as both the 4,5- and 4,6-classes of antibiotics acetylated by the WT enzyme (Table 3). Specificity constants ranged from ∼10^2 to 10^3 M^{-1} s^{-1} for this mutant due to both K_m and k_{cat} changes, compared to k_{cat}/K_m values on the order of 10^4 M^{-1} s^{-1} for WT AAC-(6′)-Ii (Table 3). Our kinetic results suggest that although AAC-Trp^{164} → Ala is somewhat impaired in the recognition and acetylation of aminoglycosides, its catalytic ability nonetheless indicates that there is one functional active site per monomer subunit, as initially evidenced by the well-defined acetyl-CoA binding pocket in the AAC(6′)-Ii binary complex structure (*10*). We therefore proceeded to dead-end inhibition studies with AAC-Trp^{164} → Ala to investigate whether the same partial inhibition observed for the AAC-(6′)Ii homodimer would be evident for this monomeric mutant.

Desulfo-CoA Inhibition Studies with AAC-Trp^{164} → Ala. Desulfo-CoA was found to be a full competitive inhibitor of the AAC(6′)-Ii reaction versus acetyl-CoA, in contrast to the partial competitive inhibition observed for the WT homodimer (Figure 3A, Table 1). As can be seen from the slope replot comparisons in Figure 7, the hyberbolic nature of the WT replot is completely alleviated when monomeric AAC-Trp^{164} → Ala is used in the inhibition studies. A K_{is} value of 39 ± 11 μM for desulfo-CoA inhibition of AAC-Trp^{164} → Ala was determined, revealing an ca. 6-fold increase in the K_{is} as compared to that determined for the WT enzyme (Table 1). Desulfo-CoA is therefore a more potent inhibitor of acetyltransferase activity when AAC(6′)-Ii is in dimeric

Table 4: Thermodynamic Parameters of the Binding of Aminoglycosides to AAC(6′)-Ii[a]

	no. of sites[b]	K_{d1} (μM)	K_{d2} (μM)	$\Delta G°_1$ (kcal/mol)	$\Delta G°_2$ (kcal/mol)	ΔH_1 (kcal/mol)	ΔH_2 (kcal/mol)	$T\Delta S_1$ (kcal/mol)	$T\Delta S_2$ (kcal/mol)
Wild-Type AAC(6′)-Ii									
neamine	2	13.0 ± 0.34	0.03 ± 0.017	−6.9	−10.7	−38.3 ± 0.8	−33.5 ± 0.1	−31.3	−22.8
kanamycin	2	3.4 ± 0.14	0.20 ± 0.012	−7.8	−9.5	−30.1 ± 0.5	−93.6 ± 2.0	−22.3	−84.0
ribostamycin	2	1.3 ± 0.07	0.06 ± 0.008	−8.4	−10.2	−44.8 ± 0.5	−81.1 ± 2.0	−36.4	−70.9
neamine + CoA	2	0.10 ± 0.013	5.8 ± 0.47	−9.9	−7.4	−21.0 ± 0.1	−11.8 ± 0.6	−11.1	−4.34
kanamycin + CoA	2	0.62 ± 0.40	65 ± 15	−8.8	−5.9	−15.8 ± 0.2	NR[c]	−7.0	NR
ribostamycin + CoA	2	0.87 ± 0.14	0.02 ± 0.003	−8.6	−10.9	−9.1 ± 0.4	−24.8 ± 0.4	−36.3	−71.0
AAC-Trp^{164}→ Ala									
neamine	1	486 ± 38		−4.7		−72.5 ± 3.7		−67.8	
kanamycin	1	833 ± 17		−4.4		−25.3 ± 0.3		−20.9	
ribostamycin	1	250 ± 5.4		−5.1		−17.3 ± 0.2		−12.1	

[a] All titrations were determined at 37 °C (310 K). [b] Refers to the number of independent binding sites for titrant as determined by the theoretical curve of best fit. [c] NR, not reported due to large error associated with the value obtained.

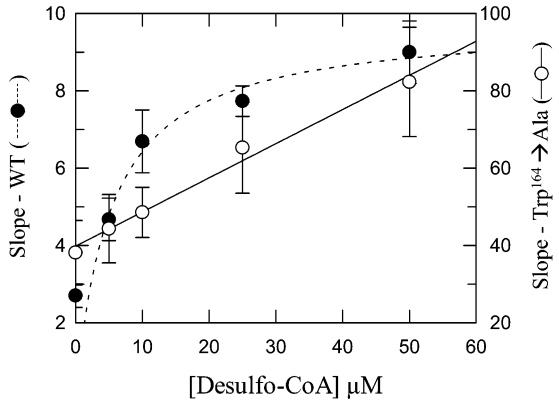

FIGURE 7: Slope replot comparisons of desulfo-CoA inhibition of wild-type and mutant AAC(6′)-Ii activity. The partial competitive inhibition revealed by the hyberbolic shape of the replot for WT enzyme (●) is not evident when the monomeric form of AAC-Trp^{164} → Ala (○) is used in dead-end inhibition studies.

form, perhaps through perturbation of acetyl-CoA binding to one monomer subunit when the second monomer subunit contains bound desulfo-CoA. This idea is also consistent with one possible explanation for the partial competitive inhibition observed for the WT dimer, which is that desulfo-CoA can bind to different sites on the homodimer (i.e., either acetyl-CoA binding site per monomer), with acetyl-CoA having a decreased affinity for enzyme if inhibitor is bound to one subunit. The result is that both free and desulfo-CoA-bound enzymes retain the ability to turnover product, if one looks at the homodimer as an "enzyme form" with two functional active sites per dimer.

Isothermal Titration Calorimetry Studies. We employed ITC studies to further investigate the binding of aminoglycosides to both WT AAC(6′)-Ii and the Trp^{164} → Ala monomer. These experiments were initiated to better understand the noncompetitive/mixed inhibition that was observed with acetylated ribostamycin, since a possible explanation was, similar to the desulfo-CoA inhibitor results, that there were unequivalent binding sites for aminoglycoside substrate per dimer. The results of our ITC experiments are summarized in Table 4, and representative ITC profiles for ribostamycin binding to WT and AAC-Trp^{164} → Ala proteins are included in Figures 8 and 9, respectively. It was immediately apparent that our titration data using WT AAC-(6′)-Ii and various aminoglycoside substrates fit best to a theoretical model describing two independent binding sites

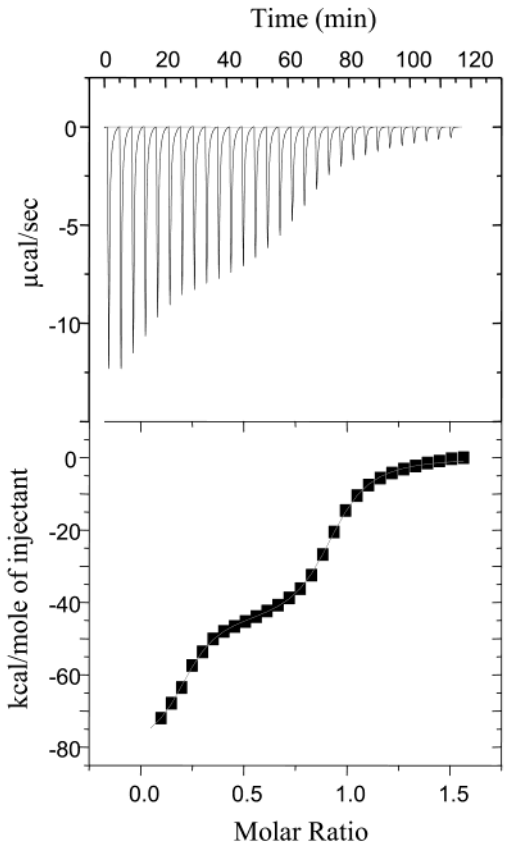

FIGURE 8: ITC profile of wild-type AAC(6′)-Ii with ribostamycin as the aminoglycoside titrant. Top: Raw experimental data from 29 automatic injections of 10 μL each of 0.7 mM ribostamycin. Bottom: Integrated titration curve showing data points (■) and the line of best fit (—) to a model describing two independent aminoglycoside binding sites per AAC(6′)-Ii dimer. ITC experimental conditions are described in Materials and Methods.

for the aminoglycoside titrant (Table 4 and Figure 8), a phenomenon which was consistent for all three representative antibiotics tested. Although a complete titration curve for WT enzyme was difficult to obtain due to the titration of multiple binding sites (see Figure 8), the K_d values with the lowest standard error (Table 4) were in the low micromolar range, in relative agreement with K_m values reported previously for AAC(6′)-Ii (*5*; Table 3). As expected from the nature of the antibiotic binding site in AAC(6′)-Ii and other aminoglycoside-modifying enzymes (*10*, *23*, *41*, *42*), our results also indicate that free enzyme can bind aminoglyco-

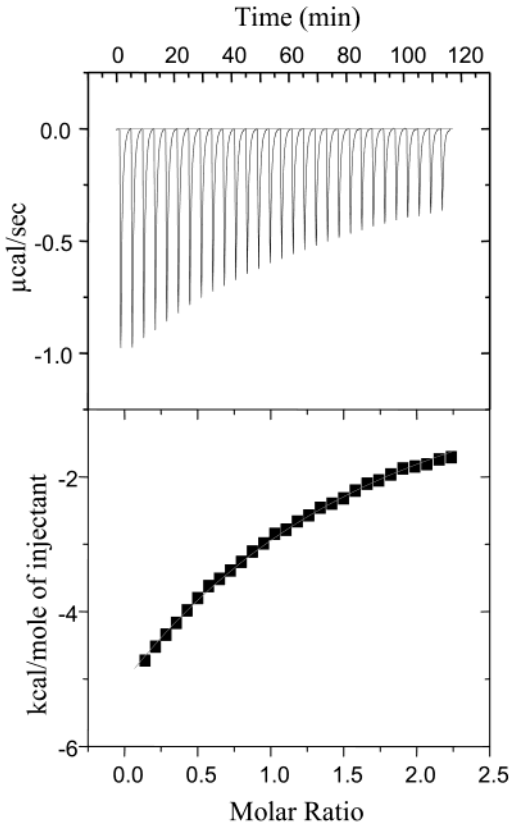

FIGURE 9: ITC profile of AAC-Trp^{164} → Ala monomer with 2 mM ribostamycin as the titrant. Experimental conditions were the same as that described in Figure 8 and in Materials and Methods. Top: Raw experimental data. Bottom: Integrated titration curve showing data points (■) and the line of best fit (—) to a model describing one binding site for the aminoglycoside titrant.

side in the absence of acetyl-CoA, generating an unproductive complex. Consistent with the numerous electrostatic interactions hypothesized to occur between protein and antibiotic based on our knowledge of the 3D structure, binding enthalpies ranged from $-\Delta H$ values of ~30 kcal mol $^{-1}$ to ~94 kcal mol^{-1} for aminoglycoside binding to free AAC(6′)-Ii (Table 4), indicating that this process is largely enthalpy driven. The aminoglycoside binding sites present per monomer are therefore not thermodynamically equivalent in the WT AAC(6′)-Ii dimer. Additional aminoglycoside titrations were performed in the presence of CoA to investigate whether the binary AAC(6′)-Ii·CoA complex would impact the thermodynamics of antibiotic binding. Again, the titration of two independent aminoglycoside sites (Table 4) made any interpretation as to whether aminoglycoside has a higher affinity for the AAC(6′)-Ii binary complex difficult.

In contrast to the results obtained for the AAC(6′)-Ii dimer, binding of aminoglycoside substrates to the AAC-Trp^{164} → Ala monomer fit best to theoretical titration curves describing only one binding site (Table 4), also seen by the representative ITC profile in Figure 9. The single K_d values reported for neamine, kanamycin, and ribostamycin for AAC-Trp^{164} → Ala were comparable to the K_m values determined for this mutant (see Tables 3 and 5), the largest discrepancy being only a 3-fold difference for kanamycin. The binding enthalpies varied from −17.3 to −72.5 kcal mol^{-1}, comparable to the range observed for the WT AAC(6′)-Ii dimer, with only slightly higher ΔG values reported (Table 4). Taken together, the ITC data for aminoglycoside binding to both WT and mutant proteins are consistent with our inhibition results and our hypothesis that the monomer subunits of the AAC(6′)-Ii dimer may "cooperate" with one another. We speculate, on the basis of the results presented here, that substrate(s) bound to one monomer subunit may affect the binding and perhaps activity of the adjacent monomer in the AAC(6′)-Ii dimer.

DISCUSSION

The inhibition and alternative substrate diagnostic studies detailed here have shown that AAC(6′)-Ii follows an ordered bi-bi ternary complex mechanism. As represented in Scheme 1, acetyl-CoA binds first followed by the aminoglycoside substrate to form a productive ternary complex. Acetylated aminoglycoside is then the first product to be released after acetyl transfer, followed by coenzyme A. The sequential ternary complex mechanism described for this acetyltransferase appears to be common for all GNAT members studied to date (*16*, *17*, *26*, *27*, *29*, *30*, *32*, *39*, *43*) and thus appears to be a universal property of this superfamily. The fact that all GCN5-related *N*-acetyltransferases share the striking structural homology centered on critical interactions with an acyl-CoA molecule suggests that these enzymes serve as catalytic scaffolds in their capacity to bind acyl-CoAs and a diverse array of other substrates to form a productive ternary complex. The ordered binding of acyl-CoA as a first substrate for many enzymes, including serotonin acetyltransferase (*17*) and histone acetyltransferases (*15*, *16*), has been complemented by observations of a protein conformational change in response to the binding of acetyl-CoA. We have also noted such changes for AAC(6′)-Ii through proteolysis studies and intrinsic protein fluorescence (results not shown), with the solvent viscosity and alternate substrate data presented here indicating that this change is a requirement for catalysis.

Product release appears to be partially rate-limiting in AAC(6′)-Ii catalysis, as evidenced by k_{cat} changes from solvent viscosity studies and solvent isotope effects. The release of the final CoA product in particular appears to account for the rate limitation in this regard, as evidenced by our inhibition studies and previous observations of substrate inhibition with numerous aminoglycosides (*5*). Of note are the significant changes in k_{cat}/K_b for aminoglycosides with increasing solvent viscosity. These results imply that the productive formation of an enzyme complex with aminoglycoside is partly limited by diffusion, in which case one would expect significantly higher specificity constants on the order of 10^7 M^{-1} s^{-1}. Since aminoglycosides have several possible conformations in solution with only one conformer optimal as a substrate, a much lower diffusion-controlled k_{cat}/K_b is possible and has been shown for an alternate aminoglycoside acetyltransferase (*39*). In contrast, solvent viscosity appeared to have no effect on the productive formation of the AAC·acetyl-CoA complex, reflected in the lack of k_{cat}/K_a changes for acetyl-CoA. A slow conformational change in the enzyme after acetyl-CoA binding is consistent with our mechanism and may also explain why no viscosity effects were observed in this case. Last, the lack of an observable solvent isotope effect confirms our viscosity results that diffusion-controlled events, and not the chemical step, largely govern k_{cat}.

The partial and mixed forms of inhibition observed during our investigation of the AAC(6′)-Ii kinetic mechanism complicated initial interpretations of our dead-end and product inhibition results. In general, the hyberbolic partial competitive inhibition observed for desulfo-CoA versus acetyl-CoA could be the result of randomness in substrate binding or could indicate that this inhibitor has more than one binding site on AAC(6′)-Ii, resulting in a catalytically active ESI complex. This latter hypothesis can also be applied to the observed mixed-type inhibition by 6′-*N*-acetylribostamycin versus aminoglycoside. We have definitively ruled out the former hypothesis of randomness in the enzyme mechanism through the alternative substrate diagnostic approach, which clearly shows that AAC(6′)-Ii follows an ordered bi-bi kinetic mechanism. The implication of our observations of partial and mixed inhibitions is that multiple binding sites exist on the enzyme for both acetyl-CoA and aminoglycoside substrates. Several pieces of evidence suggest that the physiological dimer form of AAC(6′)-Ii may act as a "functional unit" and account for the multiple binding sites hypothesized. First, the crystal structure of the AAC(6′)-Ii·acetyl-CoA binary complex (*10*) and recent structural determination for the homodimer with bound coenzyme A (*44*) reveal that there is one distinct cofactor binding site per monomer and two distinct sites per dimer. Kinetic analysis of the AAC-Trp^{164} → Ala monomer described here also indicates that each monomer subunit appears to be functional on its own, signifying single binding sites for the aminoglycoside substrate per monomer. We therefore hypothesized that the binding of substrates to one subunit may affect the binding and activity of the other subunit in the dimer, resulting in a form of cooperation between monomers and attributing to the inhibition kinetics we observed.

Consistent with our proposal of subunit cooperation in the AAC(6′)-Ii dimer, the partial nature of the competitive inhibition observed for desulfo-CoA versus acetyl-CoA was completely alleviated when the AAC-Trp^{164} → Ala monomer was used. The binding of desulfo-CoA to one active site may therefore change the affinity of the second active site for acetyl-CoA substrate, a phenomenom which may occur through a slight conformational or structural change in the dimer upon ligand binding. In addition, subsequent ITC analysis of antibiotic binding to WT AAC(6′)-Ii revealed that two nonequivalent aminoglycoside binding sites exist for the homodimer, in contrast to the one binding site characterized for the AAC-Trp^{164} → Ala monomer. Again, these results are consistent with subunit cooperation in the physiological dimer. Our ITC data also rule out the possibility of half-site reactivity of the AAC(6′)-Ii homodimer, in contrast to that observed for the aminoglycoside acetyltransferase AAC(6′)-Iy from *Salmonella enterica* (*30*, *31*). As well, previous NMR spectroscopy evidence which identified two enzyme-bound conformers for the same aminoglycoside substrate on AAC(6′)-Ii (*45*) is not inconsistent with our results. The likelihood of certain antibiotics having multiple binding modes per monomer active site, however, cannot be dismissed, given the multiple conformations possible for aminoglycoside substrates in solution.

The implications of our observations of subunit cooperativity for the AAC(6′)-Ii physiological dimer are severalfold. First, the fairly low specificity constants observed for aminoglycoside modification by AAC(6′)-Ii ($\sim 10^4\ M^{-1}\ s^{-1}$) can be partially attributed to this phenomenon if the reversible binding of ligands to each subunit effectively decreases the acetylation activity of the dimer as a whole. Second, the possibility of subunit cooperativity in other oligomeric members of the GNAT superfamily may implicate this phenomenon in the function and regulation of several enzymes, although this remains to be determined.

ACKNOWLEDGMENT

We thank Dr. Kalinka Koteva for technical assistance in the synthesis of acetylated aminoglycoside and Dr. Raquel Epand for useful discussions concerning ITC.

REFERENCES

1. Davies, J., and Wright, G. D. (1997) *Trends Microbiol. 5*, 234−240.
2. Llano-Sotelo, B., Azucena, E. F., Kotra, L. P., Mobashery, S., and Chow, C. S. (2002) *Chem. Biol. 9*, 455−463.
3. Miller, G. H., Sabatelli, F. J., Hare, R. S., Glupczynski, Y., Mackey, P., Shlaes, D., Shimizu, K., and Shaw, K. J. (1997) *Clin. Infect. Dis. 24* (Suppl. 1), S46−S62.
4. Daigle, D. M., Hughes, D. W., and Wright, G. D. (1999) *Chem. Biol. 6*, 99−110.
5. Wright, G. D., and Ladak, P. (1997) *Antimicrob. Agents Chemother. 41*, 956−960.
6. Costa, Y., Galimand, M., Leclercq, R., Duval, J., and Courvalin, P. (1993) *Antimicrob. Agents Chemother. 37*, 1896−1903.
7. Moellering, R. C., Jr., Wennersten, C., and Weinstein, A. J. (1973) *Antimicrob. Agents Chemother. 3*, 526−529.
8. Moellering, R. C., Jr., Korzeniowski, O. M., Sande, M. A., and Wennersten, C. B. (1979) *J. Infect. Dis. 140*, 203−208.
9. Wennersten, C. B., and Moellering, R. C., Jr. (1980) in *Current Chemotherapy and Infectious Disease* (Nelson, J. D., and Grassi, C., Eds.) pp 710−712, American Society for Microbiology, Washington, DC.
10. Wybenga-Groot, L., Draker, K. a., Wright, G. D., and Berghuis, A. M. (1999) *Structure 7*, 497−507.
11. Neuwald, A. F., and Landsman, D. (1997) *Trends Biochem. Sci. 22*, 154−155.
12. Angus-Hill, M. L., Dutnall, R. N., Tafrov, S. T., Sternglanz, R., and Ramakrishnan, V. (1999) *J. Mol. Biol. 294*, 1311−1325.
13. Clements, A., Rojas, J. R., Trievel, R. C., Wang, L., Berger, S. L., and Marmorstein, R. (1999) *EMBO J. 18*, 3521−3532.
14. Dutnall, R. N., Tafrov, S. T., Sternglanz, R., and Ramakrishnan, V. (1998) *Cell 94*, 427−438.
15. Rojas, J. R., Trievel, R. C., Zhou, J., Mo, Y., Li, X., Berger, S. L., Allis, C. D., and Marmorstein, R. (1999) *Nature 401*, 93−98.
16. Trievel, R. C., Rojas, J. R., Sterner, D. E., Venkataramani, R. N., Wang, L., Zhou, J., Allis, C. D., Berger, S. L., and Marmorstein, R. (1999) *Proc. Natl. Acad. Sci. U.S.A. 96*, 8931−8936.
17. Hickman, A. B., Namboodiri, M. A., Klein, D. C., and Dyda, F. (1999) *Cell 97*, 361−369.
18. Hickman, A. B., Klein, D. C., and Dyda, F. (1999) *Mol. Cell 3*, 23−32.
19. Sinclair, J. C., Sandy, J., Delgoda, R., Sim, E., and Noble, M. E. (2000) *Nat. Struct. Biol. 7*, 560−564.
20. Obsil, T., Ghirlando, R., Klein, D. C., Ganguly, S., and Dyda, F. (2001) *Cell 105*, 257−267.
21. Bhatnagar, R. S., Futterer, K., Waksman, G., and Gordon, J. I. (1999) *Biochim. Biophys. Acta 1441*, 162−172.
22. Peneff, C., Mengin-Lecreulx, D., and Bourne, Y. (2001) *J. Biol. Chem. 276*, 16328−16334.
23. Wolf, E., Vassilev, A., Makino, Y., Sali, A., Nakatani, Y., and Burley, S. K. (1998) *Cell 94*, 439−449.
24. De Angelis, J., Gastel, J., Klein, D. C., and Cole, P. A. (1998) *J. Biol. Chem. 273*, 3045−3050.
25. Lau, O. D., Courtney, A. D., Vassilev, A., Marzilli, L. A., Cotter, R. J., Nakatani, Y., and Cole, P. A. (2000) *J. Biol. Chem. 275*, 21953−21959.
26. Tanner, K. G., Langer, M. R., and Denu, J. M. (2000) *Biochemistry 39*, 11961−11969.
27. Rudnick, D. A., McWherter, C. A., Rocque, W. J., Lennon, P. J., Getman, D. P., and Gordon, J. I. (1991) *J. Biol. Chem. 266*, 9732−9739.

28. Radika, K., and Northrop, D. B. (1984) *Biochemistry 23*, 5118−5122.
29. Radika, K., and Northrop, D. B. (1984) *J. Biol. Chem. 259*, 12543−12546.
30. Magnet, S., Lambert, T., Courvalin, P., and Blanchard, J. S. (2001) *Biochemistry 40*, 3700−3709.
31. Hegde, S. S., Dam, T. K., Brewer, C. F., and Blanchard, J. S. (2002) *Biochemistry 41*, 7519−7527.
32. Williams, J. W., and Northrop, D. B. (1978) *J. Biol. Chem. 253*, 5902−5907.
33. Leatherbarrow, R. (2000) Erithacus Software, Staines, U.K.
34. Brannan, T., Althoff, B., Jacobs, L., Norby, J., and S., R. (2000) SSPS Inc., Chicago, IL.
35. Radika, K., and Northrop, D. (1984) *Anal. Biochem. 141*, 413−417.
36. Wiseman, T., Williston, S., Brandts, J. F., and Lin, L. N. (1989) *Anal. Biochem. 179*, 131−137.
37. McKay, G. A., and Wright, G. D. (1996) *Biochemistry 35*, 8680−8685.
38. Blacklow, S. C., Raines, R. T., Lim, W. A., Zamore, P. D., and Knowles, J. R. (1988) *Biochemistry 27*, 1158−1167.
39. Benke-Marti, K. M. (1987) Ph.D. Thesis, University of Wisconsin—Madison, Madison, WI.
40. Schowen, K. B. J. (1978) in *Transition States of Biological Processes* (Gandour, R. D., and Schowen, R. L., Eds.) pp 225−283, Plenum Press, New York.
41. Wright, G. D., Berghuis, A. M., and Mobashery, S. (1999) in *Resolving the antibiotic paradox: progress in drug design and resistance* (Rosen, B. P., and Mobashery, S., Eds.) pp 27−69, Plenum Publishing Corp., New York.
42. Vetting, M. W., Hegde, S. S., Javid-Majd, F., Blanchard, J. S., and Roderick, S. L. (2002) *Nat. Struct. Biol. 9*, 653−658.
43. Dyda, F., Klein, D. C., and Hickman, A. B. (2000) *Annu. Rev. Biophys. Biomol. Struct. 29*, 81−103.
44. Burk, D. L., Ghuman, N., Wybenga-Groot, L. E., and Berghuis, A. M. (2003) *Protein Sci. 12*, 426−437.
45. DiGiammarino, E. L., Draker, K. a., Wright, G. D., and Serpesu, E. H. (1998) *Biochemistry 37*, 3638−3644.

BI034148H